

## Structure of Chlorosomes from the Green Filamentous Bacterium *Chloroflexus aurantiacus*<sup>∇†</sup>

Jakub Pšenčík,<sup>1</sup> Aaron M. Collins,<sup>2</sup> Lassi Liljeroos,<sup>3</sup> Mika Torkkeli,<sup>4</sup> Pasi Laurinmäki,<sup>3</sup>  
Hermanus M. Ansink,<sup>3‡</sup> Teemu P. Ikonen,<sup>4§</sup> Ritva E. Serimaa,<sup>4</sup> Robert E. Blankenship,<sup>2</sup>  
Roman Tuma,<sup>3,5</sup> and Sarah J. Butcher<sup>3\*</sup>

Department of Chemical Physics and Optics, Faculty of Mathematics and Physics, Charles University, Prague, Czech Republic<sup>1</sup>;  
Department of Chemistry, Washington University, St. Louis, Missouri<sup>2</sup>; Institute of Biotechnology and Department of Biological and  
Environmental Sciences, University of Helsinki, Helsinki, Finland<sup>3</sup>; Department of Physical Sciences, University of  
Helsinki, Helsinki, Finland<sup>4</sup>; and The Astbury Centre for Structural Molecular Biology, University of Leeds,  
Leeds, United Kingdom<sup>5</sup>

Received 27 May 2009/Accepted 18 August 2009

**The green filamentous bacterium *Chloroflexus aurantiacus* employs chlorosomes as photosynthetic antennae. Chlorosomes contain bacteriochlorophyll aggregates and are attached to the inner side of a plasma membrane via a protein baseplate. The structure of chlorosomes from *C. aurantiacus* was investigated by using a combination of cryo-electron microscopy and X-ray diffraction and compared with that of *Chlorobi* species. Cryo-electron tomography revealed thin chlorosomes for which a distinct crystalline baseplate lattice was visualized in high-resolution projections. The baseplate is present only on one side of the chlorosome, and the lattice dimensions suggest that a dimer of the CsmA protein is the building block. The bacteriochlorophyll aggregates inside the chlorosome are arranged in lamellae, but the spacing is much greater than that in *Chlorobi* species. A comparison of chlorosomes from different species suggested that the lamellar spacing is proportional to the chain length of the esterifying alcohols. *C. aurantiacus* chlorosomes accumulate larger quantities of carotenoids under high-light conditions, presumably to provide photoprotection. The wider lamellae allow accommodation of the additional carotenoids and lead to increased disorder within the lamellae.**

Chlorosomes (5, 13) are light-harvesting complexes found in three different phyla of photosynthetic bacteria. *Chloroflexus aurantiacus* belongs to the filamentous anoxygenic phototrophs (green nonsulfur bacteria) comprising members of the phylum *Chloroflexi*. All members of the green sulfur bacteria (phylum *Chlorobi*) contain chlorosomes. Very recently, a phototropic chlorosome-containing organism was found in the phylum *Acidobacteria* (9).

Chlorosomes are oblong bodies attached to the inner side of the cytoplasmic membrane. A unique property of chlorosomes is that their main pigment, bacteriochlorophyll (BChl) *c*, *d*, or *e*, is organized in the form of an aggregate. A similar self-assembled aggregate can form in the absence of proteins and exhibits spectral and excitonic properties similar to those of pigments in the native chlorosomes (for a review, see reference 3). The BChl aggregates were suggested to form lamellar structures in chlorosomes of green sulfur bacteria with lamellar spacing between 2 and 3 nm, depending on the main BChl (BChl *c* or *e*) and the prevailing esterifying alcohol (38, 39). In this model, the lamellar layers are maintained by nonspecific

hydrophobic interactions of the interdigitated esterifying alcohols, while the in-layer arrangement is mediated through specific interactions between the stacked chlorin rings. In BChl *c*-containing chlorosomes of *Chlorobaculum tepidum* (formerly *Chlorobium tepidum*), the lamellar system (spacing, ~2 nm) often remains parallel for the whole length of the chlorosome (33, 38). In *Chlorobaculum tepidum* the lamellae exhibit considerable curvature, which was initially attributed to undulation (38), but recent end-on micrographs revealed a variety of curved lamellar structures, such as lamellar tubules or multi-layered wraps, as well as undulations (33). Recently, when chlorosomes from a *Chlorobaculum tepidum* mutant with well-ordered BChl aggregates were used as a model for electron microscopy (EM) and nuclear magnetic resonance experiments, it was proposed that BChl aggregates form concentric nanotubes with the pigments arranged in helical spirals (14).

In contrast, chlorosomes from BChl *e*-containing bacteria (e.g., *Chlorobium phaeovibrioides*) contain lamellar pigments that are organized into small domains with random orientations. It has been proposed that this arrangement improves the absorption of photons with different polarizations (39). This, together with aggregation-induced enlargement of the oscillator strength, enables the bacteria to survive under extremely low-light conditions. At this point it is unclear whether these domains also exhibit a multilayer tubular arrangement. The data suggest that while the lamellar nature of BChl aggregates seems to be conserved, the higher-order structure of chlorosomes may be different in different species.

Chlorosomes attach to the cytoplasmic membrane via a crystalline baseplate that contains BChl *a* and carotenoids and acts

\* Corresponding author. Mailing address: Institute of Biotechnology and Department of Biological and Environmental Sciences, University of Helsinki, Helsinki, Finland. Phone: 358 919159563. Fax: 358 919159930. E-mail: sarah.butcher@helsinki.fi.

† Supplemental material for this article may be found at <http://jb.asm.org/>.

‡ Present address: Free University of Amsterdam Medical Centre, Amsterdam, The Netherlands.

§ Present address: EMBL Hamburg, c/o DESY, Notkestraße 85, 22603 Hamburg, Germany.

<sup>∇</sup> Published ahead of print on 28 August 2009.

as an intermediary in energy transfer from the chlorosome to the reaction centers in the membrane. The baseplate consists of multiple CsmA protein subunits (5.7 kDa in *C. aurantiacus* and 6.2 kDa in *Chlorobaculum tepidum* [8, 27, 34, 40]). In addition to its role in energy transfer, it has been proposed that the baseplate is essential for the long-range order of lamellar BChl aggregates (2, 19). In addition to CsmA, chlorosomes of *C. aurantiacus* contain a number of other proteins, all of which are located in the chlorosome envelope (for a review, see reference 13).

Recent progress in understanding chlorosome structure has been limited to the *Chlorobi*, and it is unclear whether there is similar organization in chlorosomes from bacteria belonging to different phyla, such as the *Chloroflexi*. While *Chloroflexi* also employ chlorosomes as the main light-harvesting complex, genetically they are only distantly related to the *Chlorobi*. *Chlorobi* and *Chloroflexi* also exhibit substantial differences in the photosynthetic apparatus. The average size of chlorosomes from *C. aurantiacus*, the model organism of the *Chloroflexi*, has been reported to be smaller (100 by 30 by 15 nm) than the average size of chlorosomes from the *Chlorobi* (150 to 200 by 50 by 20 nm) (30, 32). *C. aurantiacus* chlorosomes contain a single homologue of BChl *c* (8-ethyl,12-methyl) (16) and several secondary homologues that harbor different esterifying alcohols. The main esterifying alcohol (stearol) and the minor secondary homologues have longer chains than the prevailing alcohol in *Chlorobaculum tepidum* (farnesol) (11, 16, 22).

Carotenoids are thought to play important light-harvesting and protective roles in chlorosomes (10, 13, 26, 36, 37). These hydrophobic molecules were shown to partition into the apolar space between the chlorin planes together with the aliphatic chains of the esterifying alcohols (39), and they also contribute to the hydrophobic driving force during assembly (1, 20). *C. aurantiacus* exhibits much greater variability of the carotenoid/BChl molar ratio than the *Chlorobi*. This ratio was observed to increase at most 1.4-fold in the *Chlorobi* species studied, even if the light intensity was increased more than 2 orders of magnitude (from 0.1 to 50 microeinsteins  $m^{-2} s^{-1}$ ) (6, 7). However, when there was a moderate change in the light intensity (from 400 to 2,000 lx [41] or from 44 to 127 microeinsteins  $m^{-2} s^{-1}$  [22]), *C. aurantiacus* exhibited a robust increase (fivefold) in the carotenoid content. As a result, the carotenoid content can reach levels of approximately one carotenoid molecule per two BChl molecules (41). Thus, a *C. aurantiacus* chlorosome seems to be able to accumulate significantly more carotenoids than the average *Chlorobaculum tepidum* chlorosome, which exhibits about one carotenoid molecule per 10 BChl molecules (7, 39).

In the present work we examined the overall structure, pigment arrangement, and composition of *C. aurantiacus* chlorosomes using cryo-electron tomography, X-ray scattering, and quantitative pigment analysis. *C. aurantiacus* chlorosomes appear to be thin with a distinct two-dimensional baseplate protein array. Our results also demonstrate that BChl *c* aggregates are lamellar, suggesting that this is a universal feature of chlorosome structure. The greater lamellar spacing is due to the longer esterifying alcohols and allows accommodation of more carotenoids.

## MATERIALS AND METHODS

*C. aurantiacus* J-10-fl cells were grown in DG medium (18) for 3 days in completely filled 1-liter screw-cap bottles at 50°C with an incident fluorescent light intensity on the surface of the bottles of 20 to 30 microeinsteins  $m^{-2} s^{-1}$ . Chlorosomes were prepared subsequently by using two sucrose density gradients as described by Gerola and Olson (15), except that sonication was used instead of a French press to lyse the cells. In some instances, the isolated chlorosomes appeared to aggregate and an additional sucrose gradient was employed before cryo-EM analysis. Samples for X-ray-scattering experiments were concentrated by ultracentrifugation to obtain an optical density at 750 nm of  $>200 cm^{-1}$ . The amount of residual membranes copurifying with chlorosomes was estimated from optical spectra recorded in the near-infrared region (700 to 900 nm).

Cryo-EM and X-ray-scattering data were collected as previously described (38, 39). Tilt series of low-dose images for tomographic reconstruction were recorded automatically using a Gatan Ultrascan 4000 charge-coupled device camera with the SerialEM software (25). Images were collected in 2° increments over a range of  $\pm 64^\circ$ , resulting in sampling of 0.58 nm pixel $^{-1}$ . Colloidal gold particles (10 nm) included in the sample were used as fiducial markers for image alignment. The data were binned to 2.3 nm pixel $^{-1}$  prior to calculation of tomographic reconstructions and application of a nonlinear anisotropic diffusion filter in IMOD (21). The reconstruction was rendered using Chimera (35).

To analyze the pigment composition, purified chlorosomes were dried under a vacuum and then resuspended in acetone-methanol (7:2). The mixture was vortexed and then centrifuged. The supernatant was kept, and the pellet was subjected to a second round of extraction using fresh solvent. The extraction process was repeated until the resulting pellet was colorless. The extracts were pooled and dried. All manipulations were done in the dark. Dried pigments were resuspended in 100% methanol and immediately analyzed with an Agilent 1100 high-performance liquid chromatograph (HPLC) (Agilent Technologies Inc., Santa Clara, CA) using a Zorbax Eclipse XDB-C18 reverse-phase column (particle size, 5  $\mu m$ ; 4.6 by 150 mm) with an isocratic flow rate of 100% methanol of 1 ml/min. Elution of BChls was monitored at 670 nm (BChl *c*) and 770 nm (BChl *a*), while carotenoids were detected at 480 nm. The elution profiles for various chlorosome preparations were similar and at 670 nm had four predominant peaks. Each peak was individually collected and analyzed by matrix-assisted (alpha-cyano-4-hydroxycinnamic acid) and direct-ionization, matrix-assisted laser desorption/ionization-time of flight mass spectrometry (4) using a 4700 proteomics analyzer (Applied Biosystems Inc., Foster City, CA). The molar ratios of carotenoids to BChls were computed using the areas of corresponding peaks in the chromatographs and the following extinction coefficients: 70.9  $mM^{-1} cm^{-1}$  for BChl *c*, 60  $mM^{-1} cm^{-1}$  for BChl *a* (28), 139  $mM^{-1} cm^{-1}$  for  $\beta$ -carotene, and 167  $mM^{-1} cm^{-1}$  for  $\gamma$ -carotene (47).

**Tomography data accession numbers.** The tomographic data have been deposited in the EM Data Bank under accession numbers EMDB-1642 and EMDB-1643.

## RESULTS

**Pigment analysis.** HPLC separation of chlorosome pigments allowed determination of the molar ratio of total carotenoids to total BChls (Table 1). In *C. aurantiacus* BChl *a* accounted for 5 to 8% of the total BChl content. The identities of BChl *c* homologs separated as distinct HPLC peaks were determined using mass spectrometry (see Materials and Methods) and were as follows: 8-ethyl,12-methyl BChl *c* esterified with geranylgeraniol, 9-octadecenol, and octadecanol and, unexpectedly, BChl *d* esterified with octadecanol. Note that the peak identified as BChl *d* esterified with octadecanol was a mixed peak in the HPLC analysis (results not shown). Based on the absorption spectrum of this peak, it probably coeluted with BChl *c*, as also observed by Larsen et al. (22). Thus,  $\sim 75\%$  of BChl *c* and *d* was found to be esterified with alcohols possessing a  $C_{18}$  backbone, which is greater than the 45 to 65% reported by Larsen et al. (22) and the  $\sim 65\%$  reported by Fages et al. (11). These values were shown to depend on the growth conditions (e.g., light intensity) (22), which explains the variations in the observed homolog content.

TABLE 1. Comparison of the average lamellar spacing values for chlorosomes from three species of green sulfur bacteria and *C. aurantiacus* together with relevant information from a liquid chromatography analysis of the same chlorosomes<sup>a</sup>

Species	Lamellar spacing (nm)	Lengths of esterifying alcohols	Carotenoid/BChl molar ratio	Reference(s)
<i>Chlorobaculum tepidum</i>	1.95–2.15	C <sub>12</sub> (~80%), C <sub>16</sub> (~20%)	0.08	5, 6
<i>Chlorobium phaeovibrioides</i> <sup>b</sup>	2.3–2.9	C <sub>12</sub> (~70%), C <sub>16</sub> (~30%)	0.1–0.2	6
<i>Chlorobium phaeobacteroides</i>	2.1–3.3	C <sub>12</sub> (~50%), C <sub>16</sub> (~50%)	0.25	6
<i>Chloroflexus aurantiacus</i>	2.6–4.0	C <sub>16</sub> (~25%), C <sub>18</sub> (~75%)	0.1–0.3	This study

<sup>a</sup> In *Chlorobaculum tepidum* and *C. aurantiacus* BChl *c* is the main chlorosome pigment, and in *Chlorobium phaeovibrioides* and *Chlorobium phaeobacteroides* BChl *e* is the main chlorosome pigment.

<sup>b</sup> The data are averages for the two samples evaluated.

**Absorption spectra.** Figure 1 shows the absorption spectra of two representative *C. aurantiacus* chlorosome preparations. Both samples exhibited peaks at 465 and 745 nm that originated from aggregated BChl *c* within intact chlorosomes. A weak peak around 675 nm indicated a small amount of monomeric BChl *c* or bacteriopheophytin *c*. The spectrum of one sample included prominent features at 805 and 870 nm, which were assigned to residual amounts of B806-866 light-harvesting complexes (46). These complexes reside in the underlying bacterial membrane and are not part of the chlorosome. Thus, this preparation contained a substantial amount of cellular membranes.

The relative intensity of the BChl *a* Q<sub>y</sub> band at 800 nm in the low-membrane-content sample was greater than that for *Chlorobaculum tepidum* chlorosomes. This is most likely due to the higher relative proportion of BChl *a* in *C. aurantiacus* chlorosomes (~5 to 8% of the total BChls [41; this study]) than in *Chlorobi* (~0.5 to 2% [13, 15, 39]). It also indicated that a higher proportion of the total chlorosome volume is occupied by the BChl *a*-containing baseplate (compared to *Chlorobaculum tepidum* chlorosomes); i.e., the layer of BChl *c* aggregates on top of the baseplate could be thinner. This proved to be the case and allowed us to resolve the baseplate by cryo-EM (see below).

**Cryo-EM.** Figure 2 shows two main views of chlorosomes: (i) narrower particles with a darker appearance that were apparently side views (Fig. 2a to c) and (ii) broader particles with a lighter appearance (Fig. 2d and e) that were apparently top views. In the side views the baseplate should be perpendicular

to the specimen plane, and in the top views it should be parallel to the plane. The two categories of images enabled determination of the overall dimensions of *C. aurantiacus* chlorosomes, which were typically between 140 and 220 nm long, between 30 and 60 nm wide, and between 10 and 20 nm thick. The top views have rather low contrast, which is probably due to the chlorosomes being thinner (compared to, e.g., *Chlorobaculum tepidum* chlorosomes).

A striation pattern parallel to the long axis of the chlorosomes (referred to below as “parallel striation”), similar to that observed previously for *Chlorobaculum tepidum* chlorosomes, was often observed for *C. aurantiacus* chlorosomes. However, the striation pattern was significantly more disordered than that in *Chlorobaculum tepidum* chlorosomes, which also made it less pronounced. Although the prevailing orientation of the striations was parallel to the long axis of the chlorosome, the pattern was often discontinuous. The spacing was determined by calculating Fourier transform (FT) power spectra for selected regions (Fig. 2b). The disorder led to large spacing variations in neighboring regions of the same chlorosome. The observed spacing ranged from 2.6 to 4.0 nm (mean, 3.3 nm), as determined from an analysis of more than 100 chlorosomes. Analogous to other structurally characterized chlorosomes, we attribute the parallel striation to the lamellar arrangement of BChl *c* aggregates.

The most pronounced and striking feature was observed in the top views, namely, a striation pattern perpendicular to the long axis of the chlorosome (“perpendicular striation”) (Fig. 2d and e). Consequently, the FT power spectra revealed two sets of peaks, one set originating from the parallel striation and the other set originating from the perpendicular striation (Fig. 2e). To our knowledge, such a pattern has not been observed by cryo-EM in any other green bacterium studied thus far. The perpendicular striation appeared to be very regular, and it often overshadowed the parallel striation and yielded a stronger peak in FT power spectra. The spacing of the perpendicular striation (almost always 3.3 nm) exhibited little variability between different chlorosomes. Note that while the spacing value of the perpendicular striation is identical to the mean spacing value for the parallel striation, it is easy to distinguish between the two peaks in the FT power spectra since they are located on (almost) orthogonal lines. From the analysis of the chlorosomes where peaks from both striation patterns could be resolved simultaneously, an average angle between parallel striation and perpendicular striation of 85° was determined.

In the side views, the perpendicular striation was observed

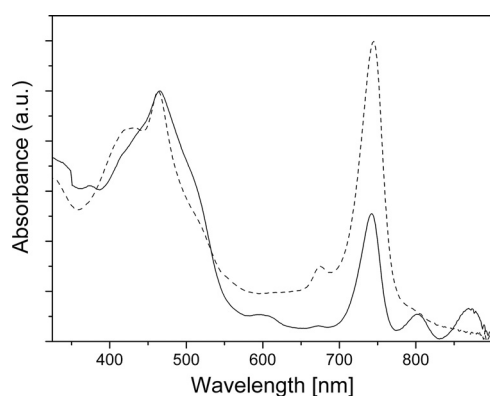


FIG. 1. Absorption spectra of the two typical chlorosome preparations, including high-membrane-content chlorosomes (solid line) and low-membrane-content chlorosomes (dashed line). The spectra were normalized at the Soret band maximum. a.u., arbitrary units.

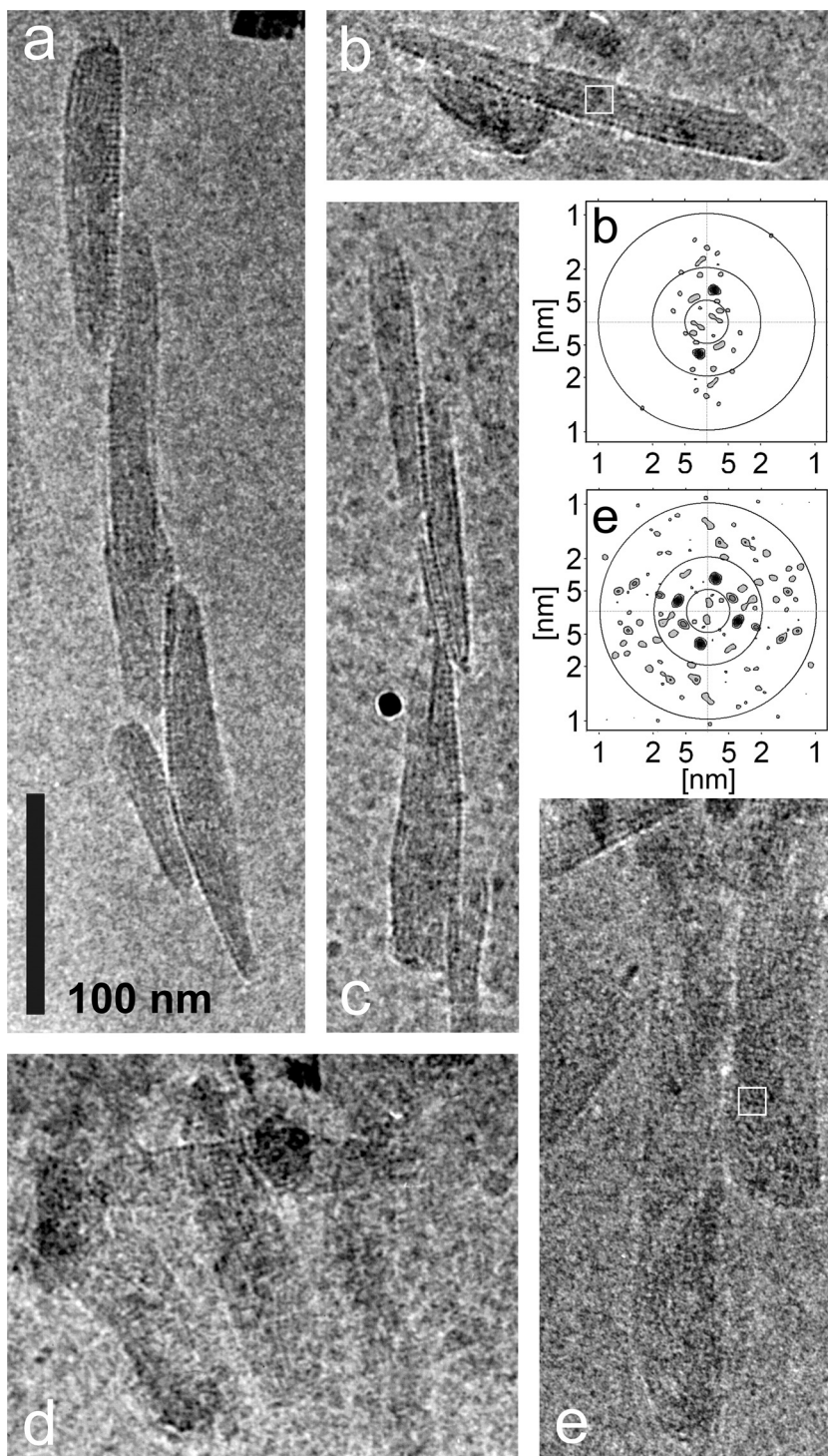


FIG. 2. Cryo-EM projections of chlorosomes from *C. aurantiacus*. (a to c) Prevailing side views. (d and e) Prevailing top views. In addition, FT power spectra for the boxed areas in panels b and e are shown. The circles indicate the distance from the center for spatial frequencies of 1, 2, and 5 nm. Micrographs were obtained at magnification of  $\times 50,000$  using the preparation with the smallest amount of membranes.

only on one side of the chlorosome (Fig. 2a). In extreme cases, when the orientation of the chlorosome baseplate was almost perfectly perpendicular to the specimen plane (Fig. 2b), the perpendicular striation merged into a line of regularly arranged dots. The spacing between the dots is 3.3 nm, which is

the same as the spacing determined for the perpendicular striation. As expected, only parallel striation was discernible from the chlorosome interior in these side projections (Fig. 2b). This indicates that the perpendicular striation originates from a planar lattice on one side of the chlorosome. Given the

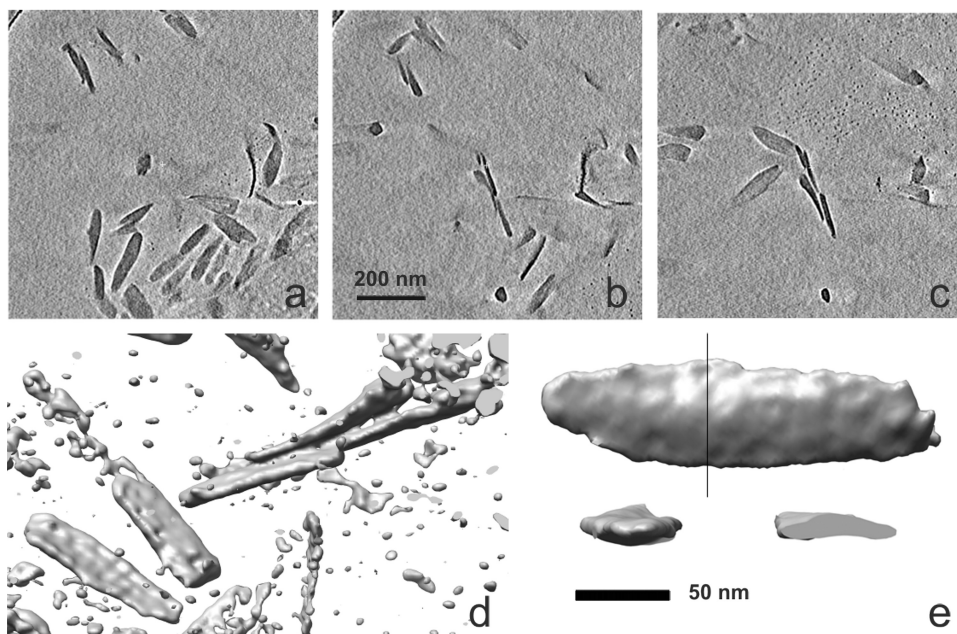


FIG. 3. Tomographic reconstruction of a field of *C. aurantiacus* chlorosomes. (a to c) Consecutive sections (thickness, 11.5 nm) through the reconstruction. (d) Isosurface view of a part of the same area shown in panels a to c. (e) Isosurface views of a subtomogram of one individual chlorosome from the top and from the side. One of the two side views is cropped to reveal a cross section of the chlorosome taken at the position of the line in the top view. The isosurfaces in panels d and e were rendered at 1.4  $\sigma$  and 1.8  $\sigma$  above the mean density, respectively.

regularity of spacing and asymmetric location, we attribute the perpendicular striation to the BChl *a*-containing baseplate (see Discussion).

**Tomographic reconstruction.** In order to confirm the chlorosome dimensions estimated from projections, we performed cryo-electron tomography. Figure 3a to c show a series of sections from a representative three-dimensional reconstruction of a volume containing several chlorosomes (see Video S1 in the supplemental material for animated views). The chlorosomes appear to be randomly distributed in the vitreous water, flat, and oblong (Fig. 3a to e). Volume rendering of well-separated chlorosomes, such as that shown in Fig. 3e, was used to estimate the chlorosome dimensions. The dimensions agreed well with those estimated from projections alone. No striation or other internal details could be observed at the limited resolution of the reconstructions. A few twisted chlorosomes were observed both in projections and in tomographic reconstructions (Fig. 3a to c; see Video S1 in the supplemental material).

**X-ray scattering.** X-ray-scattering curves had a conspicuous peak at a scattering vector magnitude ( $q$ ) of  $0.139 \text{ \AA}^{-1}$  (4.5-nm spacing; spacing =  $2\pi/q$ ) that exhibited variable intensity, which was not observed for *Chlorobi* species. This narrow peak (Fig. 4) resembled the typical diffraction from stacked lipid bilayers (45). The intensity of this peak correlated with the absorbance at 870 nm (compare the solid and dashed curves in Fig. 1 and 4, respectively), and thus this feature represents a contribution from the contaminating bacterial membrane fraction.

In addition to the membrane peak, *C. aurantiacus* chlorosomes produced a weaker and broad scattering peak at around  $0.191 \text{ \AA}^{-1}$  (3.3-nm spacing) (Fig. 4). This peak was assigned to

diffraction from the lamellar system, although it may have partially originated from the baseplate, which has the same spacing (3.3 nm). No fine structure was observed in the wide-angle region ( $q > 0.45 \text{ \AA}^{-1}$ ), presumably due to the highly disordered lamellar system, a situation similar to that in the domain-containing *Chlorobium phaeovibrioides* chlorosomes (39).

## DISCUSSION

**Overall shape and chlorosome dimensions.** The observed length (140 to 220 nm) and width (30 to 60 nm) of the *C.*

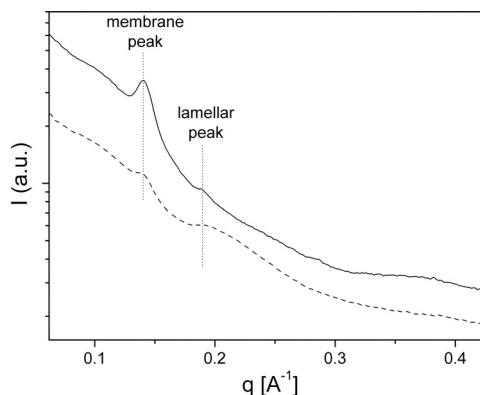


FIG. 4. X-ray scattering of chlorosomes from *C. aurantiacus*, including high-membrane-content chlorosomes (solid line) and low-membrane-content chlorosomes (dashed line). The abscissa represents  $q$ , which was determined as follows:  $q = 4\pi\sin(\theta/2)/\lambda$ , where  $\theta$  is the scattering angle and  $\lambda$  is the X-ray wavelength. I, intensity; a.u., arbitrary units.

*aurantiacus* chlorosomes were comparable to those determined for *Chlorobaculum tepidum* chlorosomes in vitreous ice (38). However, the overall dimensions reported previously for *C. aurantiacus* exhibit considerable variation (24, 30, 32), which probably reflects different cultivation conditions. In the present study we observed that the *C. aurantiacus* chlorosomes were remarkably thin (10 to 20 nm) compared to *Chlorobaculum tepidum* chlorosomes (24, 33), which explains why no apparent side and top views were resolved in cryo-EM projections of *Chlorobaculum tepidum* chlorosomes (38). The occasional appearance of twisted chlorosomes suggests that the baseplate does not have to be perfectly flat and, when necessary, it can follow the internal curvature of the cell membrane.

**Parallel striation and lamellar organization of BChl aggregates.** Based on arguments similar to those for *Chlorobaculum tepidum* (38), we attribute the parallel striation to the lamellar arrangement of the BChl *c* aggregates. The possibility that the parallel striation originated from the arrangement of envelope proteins is unlikely. According to freeze fracture EM, which is a powerful tool for studying surface features, proteins seem to be confined to the edges between chlorosomes and the cytoplasmic membrane. The envelope area adjacent to the cytoplasm exhibits no discernible substructure (42, 43). This is in contrast to the CsmA-containing baseplate of the chlorosome, which is discussed below.

Given that the parallel striation is visible in both the top and side views, the lamellae must be curved or undulate. These requirements are fulfilled by the most recent molecular model, which proposes that BChl aggregates in *Chlorobaculum tepidum* form helical stacks and further assemble into concentric multilayer nanotubes (14). The pigment layers are held together by interdigitated esterifying alcohols in the manner originally proposed for curved lamellae (38). This arrangement explains the strong circular dichroism observed for all types of wild-type chlorosomes and is also consistent with our projection images. However, the concentric, ordered nanotubes were observed mostly for chlorosomes from a mutant containing a single BChl *d* homolog (14, 33). Other types of lamellar structures, such as open curved lamellar fragments, were abundant in chlorosomes from the wild-type *Chlorobaculum tepidum* strain, which contained a mixture of BChl *c* homologues (33). Common features of all these structures are their multilayered nature, variable curvature, and considerable disorder. Thus, the concentric nanotubes represent a limiting case of perfectly ordered aggregates in chlorosomes. As observed here, the incorporation of several different longer esterifying alcohols leads to greater disorder in the lamellar arrangement in chlorosomes of *C. aurantiacus* compared to chlorosomes of *Chlorobaculum tepidum*. Due to this fact we propose that the likely arrangement of BChl *c* aggregates in chlorosomes of *C. aurantiacus* is similar to that in chlorosomes of wild-type *Chlorobaculum tepidum* (33), including the abundance of open, curved lamellar structures. Another line of evidence against the presence of intact, closed multilayered nanotubes is the thinness of the chlorosomes, which in many cases are only 10 nm thick, as revealed by tomography. This includes the baseplate (thickness, ~3 nm), so the pigment layer is roughly 7 nm thick. Given that the spacing between layers (i.e., lamellar spacing) is 3.3 nm, a nanotube with just two layers would have diameter of

over 13 nm, which is greater than the thickness of the pigment layer in such a chlorosome.

The striations in *C. aurantiacus* exhibit substantially greater spacing (~3.3 nm) than those in *Chlorobaculum tepidum* (~2.1 nm), even though BChl *c* is the main pigment in both species. However, BChl *c* in *C. aurantiacus* is esterified mainly with octadecanol (stearol), which, in the all-*trans* configuration, is 50% longer than farnesol, the major esterifying alcohol of BChl *c* in *Chlorobaculum tepidum*. A comparison of the average lamellar spacing values for chlorosomes from various species (Table 1) suggests that the lamellar spacing is roughly proportional to the average length of the esterifying alcohols. This trend is supported by our data for the *C. aurantiacus* chlorosomes, which exhibit the greatest spacing (3.3 nm) and have the longest esterifying alcohol. Thus, the results indicate that the lamellar spacing is determined primarily by the length of the esterifying alcohols.

Incorporation of longer alcohols also introduces considerable disorder, which is manifested by a wider distribution of lamellar spacing determined by EM and X-ray scattering (Table 1). Stearol does not possess any double bonds, which increases its flexibility via *trans-gauche* isomerization. This may also contribute to the observed disorder. Compared to green sulfur bacterium chlorosomes, *C. aurantiacus* chlorosomes exhibit weaker X-ray scattering from the lamellar system (Fig. 4). This is due in part to the thinness of the *C. aurantiacus* chlorosomes. As the chlorosomes are thinner, there are fewer layers that contribute to diffraction. The scattering is also weakened by the partial disorder of the lamellae, as discussed above for cryo-EM. Disorder also eliminates higher-resolution peaks ( $q, >0.45 \text{ \AA}^{-1}$ ) in diffraction, and this has been seen previously for *C. phaeovibrioides* chlorosomes, which contain smaller pigment domains (39).

It is worth noting that the chlorin ring of 8-ethyl,12-methyl BChl *c* in *C. aurantiacus* differs only in one methyl at C-20 from the chlorin ring of 8-ethyl,12-methyl BChl *d* (ignoring the esterifying alcohol), which formed very regular lamellar tubules or wraps in chlorosomes from the mutant of *Chlorobaculum tepidum* containing a single BChl homologue (14, 33). In fact, some *C. aurantiacus* chlorosome samples, including our samples, contain BChl *d* as well (22; this study). This suggests that the disorder observed for *C. aurantiacus* and some *Chlorobi* species is primarily a consequence of heterogeneity in the length of the esterifying alcohols and the larger amount of carotenoids harbored.

The lamellar spacing was shown to decrease when carotenoids were extracted from the brown (BChl *e*-containing) chlorosomes of *Chlorobium phaeovibrioides* (39). This indicates that the greater spacing is likely to accommodate more non-polar components (carotenoids and quinones). When a *C. aurantiacus* culture is exposed to higher light intensities, the amount of carotenoids in chlorosomes increases dramatically (22, 41) compared with the *Chlorobaculum tepidum* response to the same shift in growth conditions (7). The carotenoid/BChl *c* molar ratio can be from 0.09:1 to as high as 0.45:1 in *C. aurantiacus* (41), which is one of the highest ratios among all green bacteria, although it is not clear how the carotenoid content is distributed between the chlorosome interior and the baseplate. Higher carotenoid levels were also demonstrated for BChl *e*-containing chlorosomes from brown *Chlorobi* (6,

39) (Table 1). Similar to *C. aurantiacus*, the latter organisms produce BChls with long esterifying alcohols. Therefore, we propose that longer esterifying alcohols enable accumulation of larger amounts of lipophilic accessory molecules between lamellar layers. Thus, assembly of chlorosomes using longer esterifying alcohols allows *C. aurantiacus* to accumulate large amounts of carotenoids when the biosynthesis of the carotenoids is upregulated (for instance, under high-light conditions) (22, 41).

Apart from their light-harvesting and structural functions, carotenoids are known to protect photosynthetic complexes against damage caused by singlet oxygen. In contrast to *Chlorobi* species, *C. aurantiacus* is a facultatively aerobic bacterium. The expression of BChl synthesis and photosystem structural genes is suppressed in the presence of oxygen (12, 29), and therefore more efficient protection of the existing photosynthetic apparatus against singlet oxygen and radical damage may be needed. The mechanism of this modulation of gene expression is not understood, but it may be similar to that found in purple phototrophic bacteria (17). However, to our knowledge, there is no direct evidence relating the high carotenoid content to protection against oxygen. On the other hand, enhanced carotenoid biosynthesis in *C. aurantiacus* under high-light conditions, which was not observed for anaerobic *Chlorobi* species, must have a protective function rather than a light-harvesting function. Accommodation of carotenoids within the lamellar space provides an effective way to distribute and position these protective molecules close to the BChl rings without disrupting excitonic coupling.

**Perpendicular striation.** The perpendicular striation extended throughout the width of the chlorosome in top views, while in other views it was located on only one side of the chlorosome and transformed into a one-dimensional string of globular objects in the perfectly perpendicular projections. Thus, the perpendicular striation arises from a two-dimensional lattice, in contrast to the parallel striation, which reflects the projection of the three-dimensional arrangement of the BChl aggregates. This indicates that the perpendicular striation originated from the baseplate. As expected for the crystalline baseplate, the perpendicular striation appeared to be more regular than the parallel striation. We concluded that this lattice originates from a regularly arranged protein array. Similar arrays of globular features with lattice spacing ranging from 3 to 6 nm were previously observed on the interior surface of the membrane in freeze fracture replica images (42, 43). These features were assigned to the crystalline array of the CsmA protein (i.e., the baseplate). Our results are fully consistent with this interpretation, and we provide a direct estimate of the lattice constant (3.3 nm).

The side views and lattice spacing indicate that the apparent baseplate building block is an approximately spherical globule that is 3.3 nm in diameter. If we assume a globular shape and an average protein density of  $1.3 \text{ g cm}^{-3}$ , we arrive at an apparent mass of 13 kDa. The CsmA protein from *C. aurantiacus* has a monomeric mass of 5.7 kDa, and consequently the lattice building block may be a dimer. Indeed, dimeric and higher oligomeric CsmA units were observed by cross-linking for *Chlorobaculum tepidum* CsmA (23), and a recent nuclear magnetic resonance study (34) also supports the idea that a CsmA dimer is a building block of the baseplate.

Similar spacing (3.2 nm) was observed in X-ray scattering and was assigned to the baseplate in *Chlorobaculum tepidum* (19). However, the situation is more complicated for green sulfur bacteria. For *Chlorobium limicola* the 5- to 6-nm-thick crystalline layer, which connects the chlorosome to the cytoplasmic membrane, was observed in freeze fracture experiments (44). The fracture exhibited ridges with 6-nm periodicity at an angle of 40 to 60° to the long axis of the chlorosome. It was later argued that this feature might be due to the so-called FMO complex (31). Several factors make direct observation of the baseplate in *Chlorobaculum tepidum* difficult. As mentioned above, the larger amount of BChl *c* per baseplate BChl *a* molecule means that the projection images are dominated by the contribution from the lamellae. In addition, the baseplate lattice of green sulfur bacteria may be oriented at an acute angle to the long axis (i.e., to the lamellar direction), as proposed originally (44), and this further obscures the baseplate contribution to the image.

**Summary.** A consistent picture emerged from the EM and X-ray-scattering analyses. The lamellae have 2.6- to 4.0-nm spacing as determined by EM, while X-ray scattering gave a distribution with a maximum spacing of 3.3 nm, which is right in the middle of the EM range. In addition to the parallel striation, perpendicular striation is observed, which originates from the crystalline baseplate of the chlorosome. The baseplate spacing as determined by EM was 3.3 nm (and was not resolved by X-ray scattering due to overlap). Due to its crystalline character the perpendicular striation is better ordered than the parallel striation. The data presented here suggest that the length of esterifying alcohols determines the lamellar spacing, the disorder, and the amount of nonpolar components (carotenoids and quinones) that can be accommodated in the hydrophobic space of the lamellar aggregates. Lamellar expansion allows the bacterium to minimize photoinduced damage by increasing the carotenoid content at higher photon fluxes.

#### ACKNOWLEDGMENTS

This study was supported by Academy of Finland grants 1213467, 1129684, and Centre of Excellence in Virus Research 2006-2011 to S.J.B. and R.T. and grant 1118462 to R.T., by Biocentrum Helsinki (S.J.B.), by the National Graduate School in Informational and Structural Biology (T.P.I.), by the Viikki Graduate School in Biosciences (L.L.), by the Czech Ministry of Education, Youth and Sports and Czech Science Foundation (grants MSM0021620835 and 206/09/0375 to J.P.), and by U.S. Department of Energy Basic Energy Sciences grant DE-FG02-07ER15846 to R.E.B.

A.M.C. and R.E.B. thank Jianzhong Wen for assistance with mass spectrometry. We thank the Electron Microscopy Unit, Institute of Biotechnology, Helsinki University for providing facilities.

#### REFERENCES

1. Alster, J., A. Zupcanova, F. Vacha, and J. Pšenčík. 2008. Effect of quinones on formation and properties of bacteriochlorophyll *c* aggregates. *Photosynth. Res.* **95**:183–189.
2. Arellano, J. B., M. Torkkeli, R. Tuma, P. Laurinmäki, T. B. Melo, T. P. Ikonen, S. J. Butcher, R. E. Serimaa, and J. Pšenčík. 2008. Hexanol-induced order-disorder transitions in lamellar self-assembling aggregates of bacteriochlorophyll *c* in *Chlorobium tepidum* chlorosomes. *Langmuir* **24**:2035–2041.
3. Balaban, T. S., H. Tamiaki, and A. R. Holzwarth. 2005. Chlorins programmed for self-assembly. *Top. Curr. Chem.* **258**:1–38.
4. Belenky, M., B. Wang, A. Belenky, and J. Herzfeld. 2000. Monitoring of isotope substitution in cyanobacteria by matrix-assisted laser desorption ionization-time-of-flight mass spectrometry. *Anal. Biochem.* **280**:182–185.
5. Blankenship, R. E., and K. Matsuura. 2003. Antenna complexes from green photosynthetic bacteria, p. 195–217. In B. R. Green and W. W. Parson (ed.), *Light-harvesting antennas*. Kluwer Academic Publishers, Dordrecht, The Netherlands.

6. Borrego, C. M., and L. J. Garcia-Gil. 1995. Rearrangement of light harvesting bacteriochlorophyll homologues as a response of green sulfur bacteria to low light intensities. *Photosynth. Res.* **45**:21–30.
7. Borrego, C. M., P. D. Gerola, M. Müller, and R. P. Cox. 1999. Light intensity effects on pigment composition and organisation in the green sulfur bacterium *Chlorobium tepidum*. *Photosynth. Res.* **59**:159–166.
8. Bryant, D. A., E. V. Vassilieva, N. U. Frigaard, and H. Li. 2002. Selective protein extraction from *Chlorobium tepidum* chlorosomes using detergents. Evidence that CsmA forms multimers and binds bacteriochlorophyll *a*. *Biochemistry* **41**:14403–14411.
9. Bryant, D. A., A. M. G. Costas, J. A. Maresca, A. G. M. Chew, C. G. Klatt, M. M. Bateson, L. J. Tallon, J. Hostetler, W. C. Nelson, J. F. Heidelberg, and D. M. Ward. 2007. Candidatus Chloracidobacterium thermophilum: an aerobic phototrophic acidobacterium. *Science* **317**:523–526.
10. Carbonera, D., E. Bordignon, G. Giacometti, G. Agostini, A. Vianelli, and C. Vannini. 2001. Fluorescence and absorption detected magnetic resonance of chlorosomes from green bacteria *Chlorobium tepidum* and *Chloroflexus aurantiacus*. A comparative study. *J. Phys. Chem. B* **105**:246–255.
11. Fages, F., N. Griebenow, K. Griebenow, A. R. Holzwarth, and K. Schaffner. 1990. Characterization of light-harvesting pigments of *Chloroflexus aurantiacus*. Two new chlorophylls: oleyl (octadec-9-enyl) and cetyl (hexadecanyl) bacteriochlorophyllides *c*. *J. Chem. Soc. Perkin Trans.* **2791**–2797.
12. Foster, J. M., T. E. Redlinger, R. E. Blankenship, and R. C. Fuller. 1986. Oxygen regulation of development of the photosynthetic membrane system in *Chloroflexus aurantiacus*. *J. Bacteriol.* **167**:655–659.
13. Frigaard, N. U., and D. A. Bryant. 2006. Chlorosomes: antenna organelles in photosynthetic green bacteria, p. 79–114. *In* J. M. Shively (ed.), *Complex intracellular structures in prokaryotes*. Microbiology monographs, vol. 2. Springer, Berlin, Germany.
14. Ganapathy, S., G. T. Oostergetel, P. K. Wawrzyniak, M. Reus, A. G. M. Chew, F. Buda, E. J. Boekema, D. A. Bryant, A. R. Holzwarth, and H. J. M. de Groot. 2009. Alternating syn-anti bacteriochlorophylls form concentric helical nanotubes in chlorosomes. *Proc. Natl. Acad. Sci. USA* **106**:8525–8530.
15. Gerola, P. D., and J. M. Olson. 1986. A new bacteriochlorophyll *a*-protein complex associated with the chlorosomes of green sulfur bacteria. *Biochim. Biophys. Acta* **848**:69–76.
16. Gloe, A., and N. Risch. 1978. Bacteriochlorophyll *c<sub>s</sub>*, a new bacteriochlorophyll from *Chloroflexus aurantiacus*. *Arch. Microbiol.* **118**:153–156.
17. Gregor, J., and G. Klug. 1999. Regulation of bacterial photosynthesis genes by oxygen and light. *FEMS Microbiol. Lett.* **179**:1–9.
18. Hanada, S., and B. Pierson. 2007. The family Chloroflexaceae, p. 815–842. *In* M. Dworkin, S. Falkow, E. Rosenberg, K. H. Schleifer, and E. Stackebrandt (ed.), *The prokaryotes*, vol. 7. Proteobacteria: delta and epsilon subclasses. Deeply rooting bacteria. Springer, Berlin, Germany.
19. Ikonen, T. P., H. Li, J. Pšenčík, P. A. Laurinmäki, S. J. Butcher, N. U. Frigaard, R. E. Serimaa, D. A. Bryant, and R. Tuma. 2007. X-ray scattering and electron cryomicroscopy study on the effect of carotenoid biosynthesis to the structure of *Chlorobium tepidum* chlorosomes. *Biophys. J.* **93**:620–628.
20. Klinger, P., J. B. Arellano, F. E. Vacha, J. Hala, and J. Pšenčík. 2004. Effect of carotenoids and monogalactosyl diglyceride on bacteriochlorophyll *c* aggregates in aqueous buffer: implications for the self-assembly of chlorosomes. *Photochem. Photobiol.* **80**:572–578.
21. Kremer, J. R., D. N. Mastronarde, and J. R. McIntosh. 1996. Computer visualization of three-dimensional image data using IMOD. *J. Struct. Biol.* **116**:71–76.
22. Larsen, K. L., R. P. Cox, and M. Miller. 1994. Effects of illumination intensity on bacteriochlorophyll *c* homolog distribution in *Chloroflexus aurantiacus* grown under controlled conditions. *Photosynth. Res.* **41**:151–156.
23. Li, H., N. U. Frigaard, and D. A. Bryant. 2006. Molecular contacts for chlorosome envelope proteins revealed by cross-linking studies with chlorosomes from *Chlorobium tepidum*. *Biochemistry* **45**:9095–9103.
24. Martínez-Planells, A., J. B. Arellano, C. A. Borrego, C. Lopez-Iglesias, F. Gich, and J. S. Garcia-Gil. 2002. Determination of the topography and biometry of chlorosomes by atomic force microscopy. *Photosynth. Res.* **71**: 83–90.
25. Mastronarde, D. N. 2005. Automated electron microscope tomography using robust prediction of specimen movements. *J. Struct. Biol.* **152**:36–51.
26. Melo, T. B., N. U. Frigaard, K. Matsuura, and K. R. Naqvi. 2000. Electronic energy transfer involving carotenoid pigments in chlorosomes of two green bacteria: *Chlorobium tepidum* and *Chloroflexus aurantiacus*. *Spectrochim. Acta Part A Mol. Biol. Spectrosc.* **56**:2001–2010.
27. Montaño, G. A., H. M. Wu, S. Lin, D. C. Brune, and R. E. Blankenship. 2003. Isolation and characterization of the B798 light-harvesting baseplate from the chlorosomes of *Chloroflexus aurantiacus*. *Biochemistry* **42**:10246–10251.
28. Oelze, J. 1985. Analysis of bacteriochlorophylls. *Methods Microbiol.* **18**:257–284.
29. Oelze, J. 1992. Light and oxygen regulation of the synthesis of bacteriochlorophylls *a* and *c* in *Chloroflexus aurantiacus*. *J. Bacteriol.* **174**:5021–5026.
30. Oelze, J., and J. R. Golecki. 1995. Membranes and chlorosomes of green bacteria: structure, composition, and development, p. 259–278. *In* R. E. Blankenship, M. T. Madigan, and C. E. Bauer (ed.), *Anoxygenic photosynthetic bacteria*. Kluwer Academic Publishers, Dordrecht, The Netherlands.
31. Olson, J. M. 1980. Chlorophyll organization in green photosynthetic bacteria. *Biochim. Biophys. Acta* **594**:33–51.
32. Olson, J. M. 1998. Chlorophyll organization and function in green photosynthetic bacteria. *Photochem. Photobiol.* **67**:61–75.
33. Oostergetel, G. T., M. Reus, A. Gomez Maqueo Chew, D. A. Bryant, E. J. Boekema, and A. R. Holzwarth. 2007. Long-range organization of bacteriochlorophyll in chlorosomes of *Chlorobium tepidum* investigated by cryo-electron microscopy. *FEBS Lett.* **581**:5435–5439.
34. Pedersen, M. O., J. Underhaug, J. Dittmer, M. Miller, and N. C. Nielsen. 2008. The three-dimensional structure of CsmA: a small antenna protein from the green sulfur bacterium *Chlorobium tepidum*. *FEBS Lett.* **582**:2869–2874.
35. Pettersen, E. F., T. D. Goddard, C. C. Huang, G. S. Couch, D. M. Greenblatt, E. C. Meng, and T. E. Ferrin. 2004. UCSF Chimera—a visualization system for exploratory research and analysis. *J. Comput. Chem.* **25**:1605–1612.
36. Pšenčík, J., G. F. W. Searle, J. Hala, and T. J. Schaafsma. 1994. Fluorescence-detected magnetic-resonance (FDMR) of green sulfur photosynthetic bacteria *Chlorobium* sp. *Photosynth. Res.* **40**:1–10.
37. Pšenčík, J., Y. Z. Ma, J. B. Arellano, J. Garcia-Gil, A. R. Holzwarth, and T. Gillbro. 2002. Excitation energy transfer in chlorosomes of *Chlorobium phaeobacteroides* strain CL1401: the role of carotenoids. *Photosynth. Res.* **71**:5–18.
38. Pšenčík, J., T. P. Ikonen, P. Laurinmäki, M. C. Merckel, S. J. Butcher, R. E. Serimaa, and R. Tuma. 2004. Lamellar organization of pigments in chlorosomes, the light harvesting complexes of green photosynthetic bacteria. *Biophys. J.* **87**:1165–1172.
39. Pšenčík, J., J. B. Arellano, T. P. Ikonen, C. M. Borrego, P. A. Laurinmäki, S. J. Butcher, R. E. Serimaa, and R. Tuma. 2006. Internal structure of chlorosomes from brown-colored *Chlorobium* species and the role of carotenoids in their assembly. *Biophys. J.* **91**:1433–1440.
40. Sakuragi, Y., N. U. Frigaard, K. Shimada, and K. Matsuura. 1999. Association of bacteriochlorophyll *a* with the CsmA protein in chlorosomes of the photosynthetic green filamentous bacterium *Chloroflexus aurantiacus*. *BBA Bioenerg.* **1413**:172–180.
41. Schmidt, K., M. Maarzahl, and F. Mayer. 1980. Development and pigmentation of chlorosomes in *Chloroflexus aurantiacus* strain Ok-70-fl. *Arch. Microbiol.* **127**:87–97.
42. Sprague, S. G., L. A. Staehelin, M. J. Dibartolomeis, and R. C. Fuller. 1981. Isolation and development of chlorosomes in the green bacterium *Chloroflexus aurantiacus*. *J. Bacteriol.* **147**:1021–1031.
43. Staehelin, L. A., J. R. Golecki, R. C. Fuller, and G. Drews. 1978. Visualization of the supramolecular architecture of chlorosome (Chlorobium type vesicles) in freeze-fractured cells of *Chloroflexus aurantiacus*. *Arch. Microbiol.* **119**:269–277.
44. Staehelin, L. A., J. R. Golecki, and G. Drews. 1980. Supramolecular organization of chlorosome (Chlorobium vesicles) and of their membrane attachment site in *Chlorobium limicola*. *Biochim. Biophys. Acta* **589**:30–45.
45. Wilkins, M. H. F., A. E. Blaurock, and D. M. Engelman. 1971. Bilayer structure in membranes. *Nat. New Biol.* **230**:72–76.
46. Xin, Y. Y., S. Lin, G. A. Montaño, and R. E. Blankenship. 2005. Purification and characterization of the B808-866 light-harvesting complex from green filamentous bacterium *Chloroflexus aurantiacus*. *Photosynth. Res.* **86**:155–163.
47. Young, A., and G. Britton. 1993. Carotenoids in photosynthesis. Chapman & Hall, London, United Kingdom.